Highlights of Spanish Astrophysics VII, Proceedings of the X Scientific Meeting of the Spanish Astronomical Society held on July 9 - 13, 2012, in Valencia, Spain. J. C. Guirado, L. M. Lara, V. Quilis, and J. Gorgas (eds.)

Fully cosmological virtual galaxies from MASCLET

Javier Navarro-González[1], Elena Ricciardelli[1], Vicent Quilis[1], and Alexandre Vazdekis[2]

[1] DAA, Universitat de València, Spain
[2] IAC, La Laguna (Tenerife), Spain

Abstract

We present the study of the most massive galaxies ($M^* > 10^{11}\,\mathrm{M}_\odot$) found in a cosmological simulation performed with MASCLET (Mesh Adaptative Scheme for CosmologicaL structurE evoluTion) and analyzed with HALMA (HALo finder for MAsclet). We focus on the structure of these virtual galaxies, analysizing their radial gradients, morphology, kinematics and chemical characteristics. By classifying galaxies depending on their merging history, morphology or kinematics we have found that the most relevant differences in the profiles appear when they are separated according to their merging history. We suggest that some of those differences could be explained due to the spatial segregation of the stellar populations formed in-situ and ex-situ.

1 Introduction

One of the most hot topics in Cosmology is how the galaxies, the building blocks of the Universe, are formed. The hierarchical ΛCDM model, the most accepted nowadays, tells us that the small galaxies merged to form larger galaxies. One important ingredient of this forming scenario is the number and the size of galaxies needed to produce a bigger one. Numerical simulations could answer some of these open questions and try to find coincidences with observational plane. One of such issues is the size evolution of compact massive galaxies (1 kpc) from $z > 2$ to nowadays. These systems look like typical elliptical galaxies but with sizes from two to five times their original sizes at $z > 2$ (e.g. [11, 1, 2]). A feasible explanation of the change in the properties of these systems relies on a two phases scenario. At the beginning, $6 > z > 2$, there would be a rapid phase of in-situ star formation, leading to the formation of the galactic cores. Later on, $z < 2$, when the galaxies run out of gas, a second phases stars up when several minor mergers events take place. Such minor mergers leave lots of stars in the outer part of the galaxies [5, 6] producing the size evolution. In this contribution, we analyze the most massive well resolved galaxies in an AMR fully cosmological simulation performed with MASCLET, according to their merger history, morphological and dynamical properties and the separation of the stellar populations profiles into stars formed in-situ and ex-situ.

2 Numerics

2.1 Simulation

The simulation used for this study was performed with the cosmological code MASCLET [8]. This code couples an Eulerian approach based on *high-resolution shock capturing* techniques for describing the gaseous component, with a multigrid particle mesh N-body scheme for evolving the collisionless component (dark matter). Gas and dark matter are coupled by the gravity solver. Both schemes benefit of using an adaptive mesh refinement (AMR) strategy, which permits to gain spatial and temporal resolution.The initial conditions were set up at $z = 50$ for a cube of comoving side length of 44 Mpc. The computational domain was discretized with 128^3 cubic cells. A maximum of 7 levels of refinements has been used, which gives a maximum physical spatial resolution of 2.7 kpc. Our simulation includes cooling, heating process, star formation, and stellar feedback following the ideas of [13], and [10]. The numerical simulation was run with the following cosmological parameters: $\Omega_{\rm m} = 0.25$, $\Omega_\Lambda = 0.75$, $H_0 = 73$ km s^{-1} Mpc^{-1}, $n_{\rm s} = 1$ and $\sigma_8 = 0.8$.

2.2 Halo finder

The outcome of our simulation is a complete description of the three components included in the simulation, namely, gas, dark matter and stars. In order to analyse and characterize the properties of the galaxies at the different outputs, we identify the galaxies by means of an adaptive friends of friends algorithm applied only to the star particles. In the practical implementation of our finder, we linked star particles using an iterative process starting from a large linking length of $\sim$ 10 kpc and reducing it until a limit length of $\sim$ 2 kpc. Once all the particles belonging to a give halo are identified by the iterative linking process, they undergone an extra process to check whether they are gravitationally bound to the systems. Those unbounded particles are drop off the list of member of such galaxy.

The result of the halo finding process is a complete sample of all the galaxy-like objects in our simulations at the different redshifts. Every galaxy is perfectly defined and all its properties determined, therefore, the generated catalogue can be used to explore the properties of galaxies and to compare with the observational plane. By tracking back in time the merging history of the simulated galaxies, it is possible to identify the main progenitor of all galaxies at the present time.

2.3 The sample and the synthetic observational data

We focus our analysis on the more massive galaxies ($M_* > 10^{11}$ M$_\odot$), which are also the best resolved objects in the simulation. Galaxies in the process of merging are excluded from

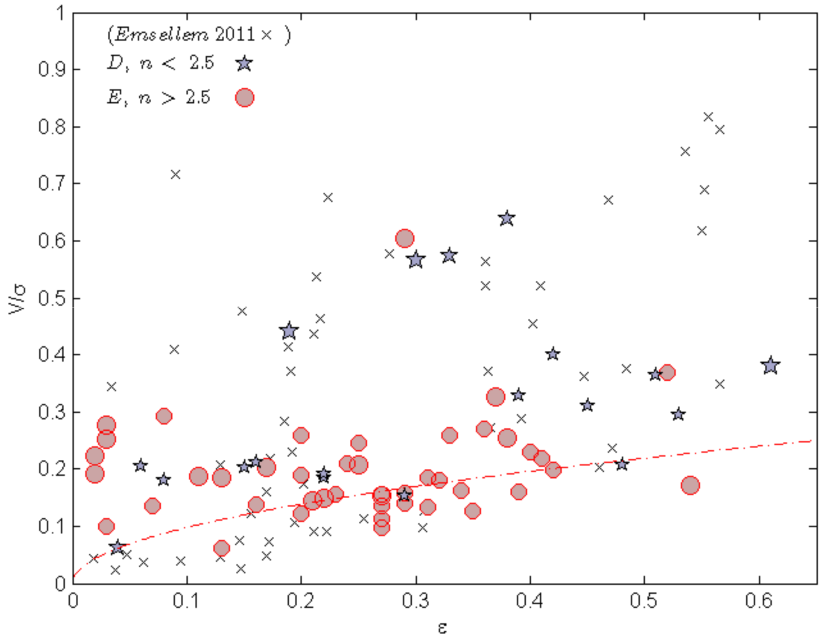

Figure 1: Morphological distribution of our galaxies sample (circles represent elliptical-like, and stars show disk-like) comparing with observational brightest ATLAS galaxies (crosses) from [3]

the analysis, as their dynamical and morphological state are far from being relaxed, hence difficult to characterize. We have therefore selected only galaxies that have not suffered a merger in the two previous snapshots of the simulation, corresponding to about ~ 1 Gyr. After that, we obtain a sample of 21 independent well resolved objects. In order to treat our simulated galaxies as close as possible to real objects, the 3-D structure of a galaxy has been converted in a 2-D map by projecting its volume of star particles onto a plane. We chose a mesh whose pixels have a fixed comoving size of 2.7 kpc. To convert physical quantities in observables we adopt the MIUSCAT stellar population synthesis models [12, 9] and assign a spectrum to each particle by choosing the model having age and metallicity closest to those of the star particle.

Artificial images have been created by projecting along three projection axis, obtaining 63 objects to analyze (see Fig. 1). The structural parameters are measured through the two-dimensional fitting code GALFIT [7] .

3 Analysis

We study the sample of the most massive galaxies and their more relevant features attending to three wide criteria: (i) their dynamical properties, (ii) their evolutionary history, and (iii) their morphologies. As first step, we classify the galaxies in our sample according to the dynamics. To do so, we look at a quantity widely used in the literature (e.g. [3]): the ratio of the rotational velocity to the dispersion velocity (v/σ). This quantity allows us to split the sample into two groups, the slow rotators and the fast rotators objects. The second criteria that we use to study the galaxies in our sample is their evolutionary history. Thus, according with their evolution, we separate the galaxies in two categories: those galaxies which have suffered at least a merger event , and those other galaxies that have a quiet evolution without relevant mergers. Finally, the third criteria use to sort the sample is the morphology. The basic methodology consist in fitting the light profile of each object by the corresponding Sérsic profile and obtain the Sérsic index (n). We use n index to discriminate between early-type ($n > 2.5$) and late-type ($n < 2.5$) galaxies.

3.1 1D profiles

One dimensional (1D) profiles are useful tools to compare the results of the simulations with observational data. We obtain profiles according to the three criteria, and we note there are substantial differences between those objects which have had a relatively quiet life and those involved in major merger processes (see Fig. 2).

The evolutionary history of the galaxies turns out be an important factor to shape the present-day structure of the galaxies. We can see, galaxies having undergone an important merger tend to have lower Sérsic indices, higher stellar mass (and hence higher velocity dispersion at all radii) and higher rotational velocities, mainly in the outer radii. They are also younger (younger ages at all radii) and steeper metallicity gradients than the quiet counterpart. The reason for this is that most of the mergers suffered by our simulated galaxies are dissipational (strong star formation induced by the merger), hence producing a rejuvenation of the stellar population content in the central region.

3.2 Star formation history: in situ versus accreted

In order to study the star formation history of the simulated galaxies, we have separated the stars formed in the main progenitor (in-situ) from those accreted later on from mergers or smooth accretion. Figure 3 shows median profiles of the mass distribution for three representative merger and quiet galaxies, chosen in order to have similar stellar masses. Both type of galaxies appear dominated by accreted stars, whereas just a minority of stars have been formed in-situ. Indeed, 80%–90% of the zero-redshift stellar mass is in accreted stars and only 20%–10% have been formed in-situ. The two profiles differ mostly in the case of quiet galaxies. We can see in the central part of these galaxies, a in-situ SSP profile much more steeper than in the case of merger galaxies.

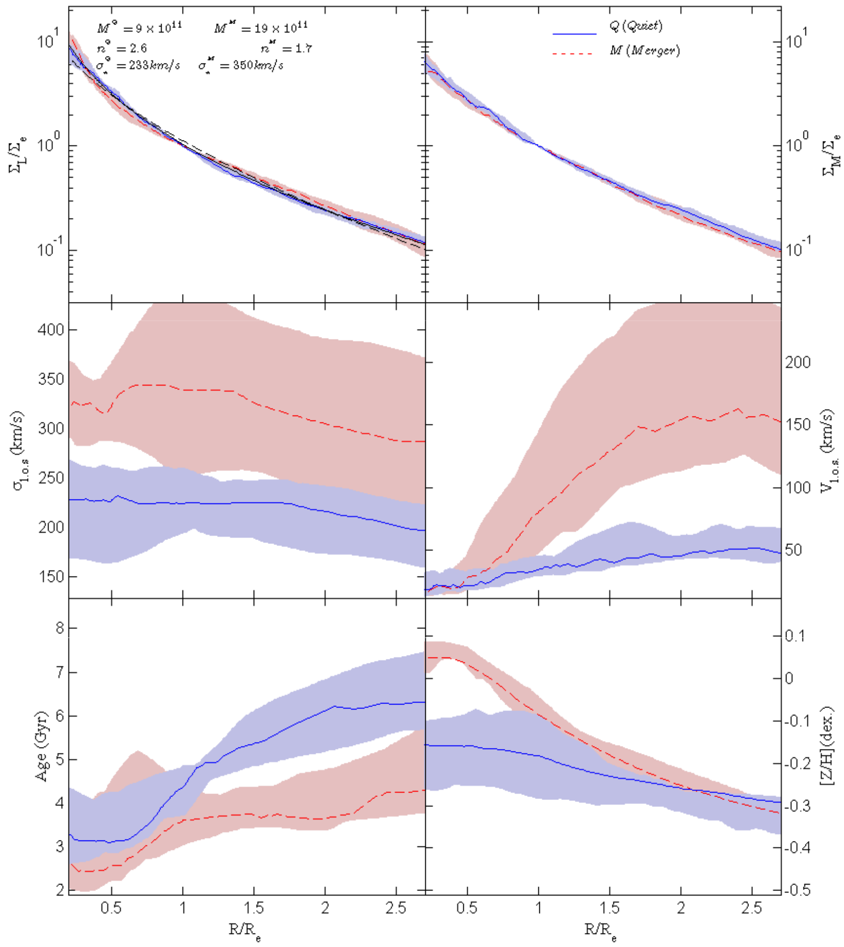

Figure 2: 1D median profile of galaxies grouped according with their evolutionary history. Lines represent the median of all the profiles of the galaxies in the group and the shaded regions stands for the $25^{\text{th}}/75^{\text{th}}$ percentile of the distribution. The panels represent: luminosity (*top left*), surface density (*top right*), velocity dispersion (*middle left*), line of sight velocity (*middle right*), light-weighted age (*down left*), and metallicity (*down right*). The blue continuous line and the blue shaded region correspond to quiet objects (Q), whereas the red dashed line and the shaded region stand for the objects which have suffered at least a merger event. In order to average all the profiles corresponding to the galaxies, the radial profile of each galaxy is rescaled to its effective radius, R_{eff}.

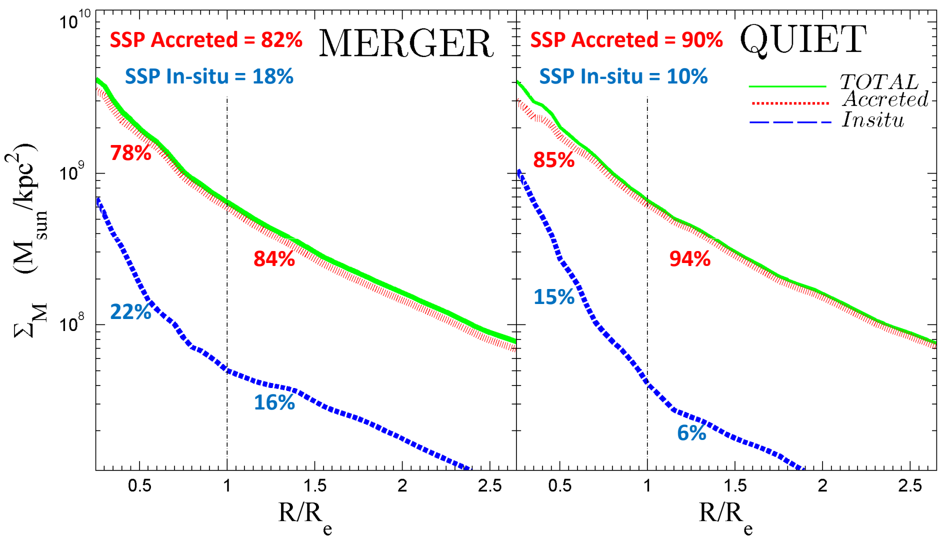

Figure 3: Median mass density profiles for three merger (*left*) and three quiet (*right*) galaxies. The two subsamples have been chosen in order to have similar mass ranges. The contributions from stars formed in-situ and accreted are shown by the dashed and dotted lines respectively. In the top of the panels, we can see fraction of accreted SSP and in-situ SSP in each of the two subsamples. Inside each one of those panels, we show fraction of accreted SSP and in-situ SSP, top and bottom respectively, studying separately the central part of the galaxy (inside $R_{\rm eff}$) and the outer part of the galaxy (outside $R_{\rm eff}$).

The dominance of the accreted SSP in both, merger and quiet galaxies, seems in agreement with the findings of [6] and [4]. We find that the outermost part of massive galaxies has been shaped by continuous accretion.

References

[1] Buitrago, F., Trujillo, I., Conselice, C. J., et al. 2008, ApJ, 687, L61

[2] Cenarro, A. J. & Trujillo, I. 2009, ApJ, 696, L43

[3] Emsellem, E., Cappellari, M., Krajnović, D., et al. 2011, MNRAS, 414, 888,

[4] Lackner, C. N., Cen, R., Ostriker, J. P., & Johansson, P. H. 2012, ApJ, 744, 63

[5] Oser, L., Ostriker, J. P., Naab, T., Johansson, P. H., & Burkert, A. 2010, ApJ, 725, 2312

[6] Oser, L., Naab, T., Ostriker, J. P., & Johansson, P. H. 2012, ApJ, 744, 63

[7] Peng, C. Y., Ho, L. C., Impey, C. D., & Rix, H.-W. 2002, AJ, 124, 266

[8] Quilis, V. 2004, MNRAS, 325, 1426.

[9] Ricciardelli, E., Vazdekis, A., Cenarro, A. J., & Falcón-Barroso, J. 2012, MNRAS, 424, 172

[10] Springel, V. & Hernquist, L. 2003, MNRAS, 339, 289

[11] Trujillo, I., Förster Schreiber, N. M., Rudnick, G., et al. 2006, ApJ, 650, 18

[12] Vazdekis, A., Ricciardelli, E., Cenarro, A. J., et al. 2012, MNRAS, 424, 15

[13] Yepes, G., Kates, R., Khokhlov, A., & Klypin. A. 1997, MNRAS, 284, 235